Pacific Northwest
NATIONAL LABORATORY

PNNL-29702

Polarization Imaging for International Safeguards

Fiscal Year 2019 Report

February 2020

M Bliss
BE Bernacki
KA Kaplan

U.S. DEPARTMENT OF ENERGY

Prepared for the U.S. Department of Energy
under Contract DE-AC05-76RL01830

DISCLAIMER

PACIFIC NORTHWEST NATIONAL LABORATORY
operated by
BATTELLE
for the
UNITED STATES DEPARTMENT OF ENERGY
under Contract DE-AC05-76RL01830

Printed in the United States of America

Available to DOE and DOE contractors from the
Office of Scientific and Technical Information,
P.O. Box 62, Oak Ridge, TN 37831-0062;
ph: (865) 576-8401
fax: (865) 576-5728
email: reports@adonis.osti.gov

Available to the public from the National Technical Information Service
5301 Shawnee Rd., Alexandria, VA 22312
ph: (800) 553-NTIS (6847)
email: orders@ntis.gov <https://www.ntis.gov/about>
Online ordering: http://www.ntis.gov

Polarization Imaging for International Safeguards

Fiscal Year 2019 Report

February 2020

M Bliss
BE Bernacki
KA Kaplan

Prepared for
the U.S. Department of Energy
under Contract DE-AC05-76RL01830

Pacific Northwest National Laboratory
Richland, Washington 99354

This page intentionally left blank.

Abstract

A polarization imaging camera, Salsa (Bossa Nova Technologies) was evaluated for use in nuclear safeguards inspection with a focus on swipe sampling. The camera and supporting electronics and software determine the full Stokes parameters for the entire image field. The camera can be used for real-time video or still images. Stokes parameters S0, S1, S2, and S3 can be recorded for each pixel and exported for post processing.

This study compared color photography to polarization imaging for powders on many surfaces under ambient lighting. False color images can be created from the Stokes parameters directly from the vendor software to highlight the various polarization states. In most cases, linear polarization showed the greatest effects.

The polarization images are easy to collect and very sensitive to surfaces and textures. Fine powders are highlighted in the images, and particle size and refractive index effects were noticed. The images are not affected by ambient lighting (angle, or intensity). Lens choice is key and may require expert knowledge. Very small deposits of 1 µm particles were difficult to image using the standard video lens. General dirt on smooth surfaces and handprints are easily documented as well as powders on textured painted surfaces. Scratches on metal surfaces can be readily separated from other image features. The camera may be useful for tamper indication as surface damage is easy to discern and ambient lighting is not a concern.

This page intentionally left blank.

Summary

International Atomic Energy Agency inspectors need to be efficient while at a facility. Currently inspectors rely on extensive training and facility knowledge when deciding where to take swipe samples. Polarization imaging can highlight anomalous sites for swiping. It can also be used to inspect for scratch marks or tampering of equipment enclosures. Commercial polarization imagers are typically used to determine surface finish quality and homogeneity. These imagers weigh as little as 500 g.

Polarization imaging is separated into two categories: division of time, and division of amplitude. Recently available division of amplitude approaches exploit a super-pixel of the image that is divided into four sub-pixels at different polarization angles. The reflected and scattered light can be separated to characterize surfaces and any deposits on them. Polarization imaging enhances features in low-light conditions because it is based on scattering and the changes in polarization states, and not solely intensity.

This study procured and evaluated the Salsa (from Bossa Nova), a commercial polarization imager that uses standard commercial camera lenses. The camera is an excellent documentation tool for industrial settings because ambient light effects can be negated, and clean and dirty surfaces are readily differentiated. The Bossa Nova Salsa polarization imager uses electrically controlled liquid crystal filters to polarize the light collected in a division of time approach. Sequential images are analyzed to determine the Stokes polarization parameters for still images or video. Pixel-by-pixel polarization information can be stored for later analysis.

Other systems considered use linearly polarized sub-pixels. These cameras are generally faster for image collection but did not offer all polarization states essential to a detailed evaluation and were not as mature as the Salsa system.

The Salsa system came with user and software developer manuals, control software, and graphical user interface. The camera accepts standard lenses via the industry-standard C-mount or Nikon lenses using a F-to-C mount adapter. Optical filters for red, green, and blue light are supplied to minimize uncertainties in the polarization measurement. Of the four vendors contacted, Bossa Nova Technologies offered the most complete system with real-time video and digital image output for all four Stokes parameters. The hardware consists of the camera, camera and liquid crystal controller and a portable computer.

Initial testing confirmed that no special lighting was required for the camera to function well. The angle and height of the camera to the surface being imaged can be varied greatly and is not critical to operation. The detector gain should be adjusted to avoid pixel saturation. The green and blue filters gave the best polarized images. Only 10 frames can be co-added in a still image. Co-adding frames did improve the images. The user must select what polarization information to save for each image. The four polarization parameters are not automatically saved.

Mathematica scripts were written to display the images as black and white or false color, based on the number of polarization parameters selected. The real-time video was useful in selecting camera angle and height. Video mode to the camera control computer was useful in scanning a room or zone for interesting areas to take more detailed still images.

Powder smears were readily detected in the images, especially, smears that were not apparent to the eye or conventional intensity-only cameras. The polarization signatures from powders

were strong compared to the surroundings. Scratches and fingerprints were visible on horizontal and vertical surfaces. Sandpaper was used to test the imager’s response to particle size and texture. Fine grades of sandpaper had different polarization signatures down to 10-µm grit independent of viewing and lighting angles. White powders with different refractive index appear different from each other as do different particle sizes of the same materials. Generally, for thin materials where the light can be reflected, back through the particle, refractive index and thickness have equal importance and one must be known to determine the other.

The polarization data from the images can be transferred to other software for further analysis. Mathematica scripts were written to transfer the data to other programs. Pacific Northwest National Laboratory (PNNL) used ENVI for post processing. ENVI was developed for remote sensing applications and is widely applied to image data. The Salsa images were compared to processed images to determine if more information about the image area could be revealed.

PNNL found the Salsa camera easy to operate and it performed well under ambient light. For viewing large areas such as the laboratory hood sill, the imager readily showed that the surface was dirty. Close examination of the images showed corrosion and handprints and generally dusty surfaces which may be of aid during facility inspections in determining areas for swipe sampling. The advantage of the camera over the unaided eye is in showing powders on textured or painted surfaces. The polarization images accentuated fine powders on a variety of surfaces and indicated differences between assorted white or colorless chemical powders.

The polarized images readily resolve and highlight surface defects such as scratches and corrosion. The field-of-view, as well as magnification of the camera is determined by the lens choice, which is extensive, especially for F-mount lenses. The images may offer an advantage in documenting swipe locations because ambient lighting has little effect on the images. Although the imager did not resolve small deposits (mm scale) of 1 µm uranium oxide particles on a glass slide, this could be addressed through judicious choice of fore-optics. However, this may not be the best use of the inspector’s time. Thus, for very small particle sizes using the camera for swipe sample location may not be worthwhile without further investigation and lens evaluations. The camera appears to be suitable for tamper indication and removing glare from water in cooling or storage ponds or glove box windows (Figure S.1).

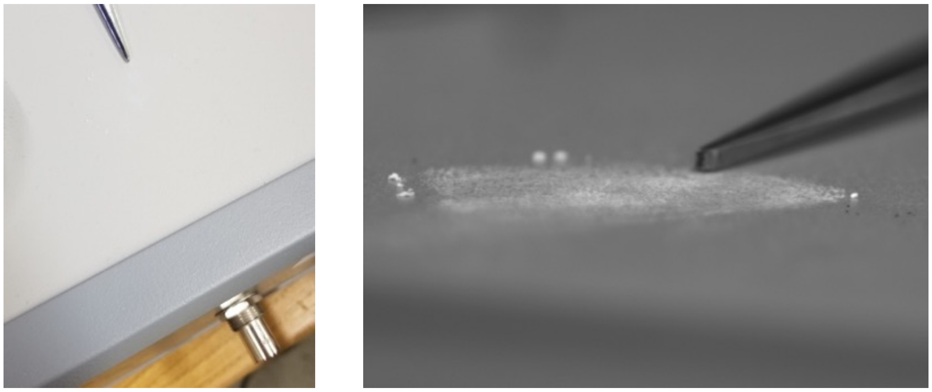

Figure S.1. Neodymium Oxide powder on a Painted Metal Surface; (left) visible light photograph, (right) polarized light image. The metal pointer is in the same position in both images.

Acknowledgments

The authors acknowledge the funding from DOE NNSA NA-241 and the Safeguards Student Internship Program.

This page intentionally left blank.

Acronyms and Abbreviations

DOLP	degree of linear polarization
DOCP	degree of circular polarization
fps	frames per second
IAEA	International Atomic Energy Agency
S0	Stokes parameter for intensity of polarized light
S1	Stokes parameter for the difference between the intensity of vertically and horizontally polarized light
S2	Stokes parameter for the difference between the intensity of light polarized at +/- 45 °
S3	Stokes parameter for the intensity difference between right- and left-handed circularly polarized light

This page intentionally left blank.

Contents

Abstract iii
Summary v
Acknowledgments viii
Acronyms and Abbreviations x
Contents xii
1.0 Introduction 1.1
2.0 General Images 2.1
2.1 General Outdoor Images 2.1
2.2 General Indoor Images 2.2
3.0 Powder Images 3.1
4.0 Semiquantitative Images 4.1
5.0 Uranium Oxide Particles 5.1
6.0 Conclusions 6.1
7.0 Bibliography 7.1
Appendix A Camera Parameter Tests A.1

Figures

Figure 1.1. Salsa Camera System....1.2
Figure 2.1. Schematic of Polarized Light Traveling out of the Page Toward the Reader. 2.1
Figure 2.2. (From left to right) S0, S1, S2, and S3 Polarization Images of the Same Scene. 2.3
Figure 2.3. Data from the images in Figure 2.2 combined as false colors....2.3
Figure 2.4. Principle Components Analysis of Salsa Images using ENVI Software Showing Greater Detail than the Pure Stokes Images. 2.4
Figure 2.5. False Color Image Created from the Principle Components Images using ENVI Software. 2.4
Figure 2.6. S0, S1 and S2 (left to right) Images of a Laboratory Chemical Hood Sill (blue filter)....2.5
Figure 2.7. From left to right, S0, S1, and S2 Images of a Laboratory Hood Sill. 2.6
Figure 2.8. Images Before (left column) and After (right column) Adding a Fingerprint to the Metal Sill. 2.7
Figure 2.9. Comparison of Black and White and Color Images. 2.8
Figure 3.1. Neodymium Oxide on a Painted Electrical Box....3.1
Figure 3.2. False Color Images of Neodymium Oxide Powder on the Metal Hood Sill. 3.2
Figure 3.3. ENVI-processed Images Using the Salsa Output. 3.2
Figure 3.4. ENVI-processed Image Using Multivariante Image Analysis. 3.3
Figure 4.1. (Left to right) S0, S1, S2, and S3 of Various Sandpapers with the Grit Size Handwritten on Lined Paper (120, 240, 600, and1500). 4.2
Figure 4.2. The Same Four Sandpapers as in Figure 4.1 with Supplemental Lighting. 4.3
Figure 4.3 The Four Sandpaper Squares at Different Orientations Under Ambient Lighting. 4.4
Figure 4.4 The polarization of Lithium Carbonate and Magnesium Oxide are Distinctly Different from each Other and the Blank Sandpaper. 4.5
Figure 4.5. The columns (from left to right) show S0, S1, S2 and S3 images of 240 Grit Sandpaper Smeared with Lithium Carbonate, Cerium Oxide (center), and Magnesium Oxide. 4.6
Figure 4.6. 240 Grit Sandpaper Smeared with Lithium Carbonate, Neodymium Oxide and Magnesium Oxide. 4.7
Figure 4.7. Silica and Alumina Smears on Sandpaper Sorted by Particle Size. 4.8
Figure 4.8. Post-processed False Color Images of the Smears in Figure 4.7. ....4.9
Figure 5.1. Uranium Oxide Particles on a Glass Slide. 5.1

1.0 Introduction

International Atomic Energy Agency (IAEA) inspectors work in complex industrial environments and rely heavily on facility familiarity. This project is intended to determine if an advanced imaging tool, a polarization imager, can be an aid to inspectors.

Polarization imaging reveals the interaction of ambient light with various surfaces and materials. Light is reflected and scattered from surfaces depending on its polarization state. Changes in polarization reveal texture, coatings, dirt, scratches, etc. Polarized sunglasses allow the wearer to filter out horizontally polarized light that has reflected off smooth surfaces, known as glare. Rotating polarizing sunglasses 90° selects the glare over the non-reflected light.

Polarization imagers are used as quality control inspection tools for coatings and paint. Polarization information reveals the curvature of surfaces and can be used to reveal design details for reverse engineering structures. Polarization imaging is also used to view objects through fog or smoke that scatters light. These imagers can be used to see beyond surface glare into water or other transparent materials such as glass windows. Mechanical strain in transparent and semi-transparent materials can be quantified by measuring optical polarization. Polarization imagers can reveal shape and texture under low-light conditions when the unaided human eye cannot.

Flash photography can result in images dominated by glare, and glare from bright lighting can make surface inspections difficult. Polarization images have improved contrast over conventional images, especially of dark or poorly lit objects. Polarization images also can remove effects from shadows and poor ambient light and improve low contrast images.[1] In general, polarization imaging can be exploited as an anomaly detector that highlights structured or man-made features over those having fractal characteristics. This study seeks to determine the relevance of polarization imaging to safeguards facility inspections.

This project contacted several vendors seeking a complete system that measured all the Stokes polarization parameters and had operating software with a good user interface. 4D Technologies, Polaris Sensor Technologies and Bossa Nova Technologies all offered systems. Bossa Nova Technologies' Salsa system was the most complete as the other venders offered custom-built systems that would have required significant software development. Also, the Salsa camera system was made to give all four Stokes parameters (S0, S1, S2, and S3) whereas the other cameras did not determine the S3 parameter (circularly polarized light). The Salsa system had extensive user documentation and software development manuals, which the other vendors did not offer. The Salsa camera system uses a liquid crystal polarizer that is controlled by an electric field. Other cameras are based on sensors that measure four polarizations simultaneously in sub-pixels. This method is faster, but the sensor is specially fabricated and is much more expensive. The Salsa image rate of 12 frames per second (fps) is adequate for real-time video. The camera came with a prime focus video lens that performed well for panning rooms and then examining surfaces from a short distance (<1 m), and any C-mount lens could be used along with better-quality F-mount (Nikon camera mount) lenses via an F-to-C mount adapter that was purchased with the system (Figure 1.1).

[1] The effects of polarization are best described visually. A video that demonstrates these effects is https://www.youtube.com/watch?time_continue=2&v=C5hhKcMYRGI (Accessed February 6, 20120).

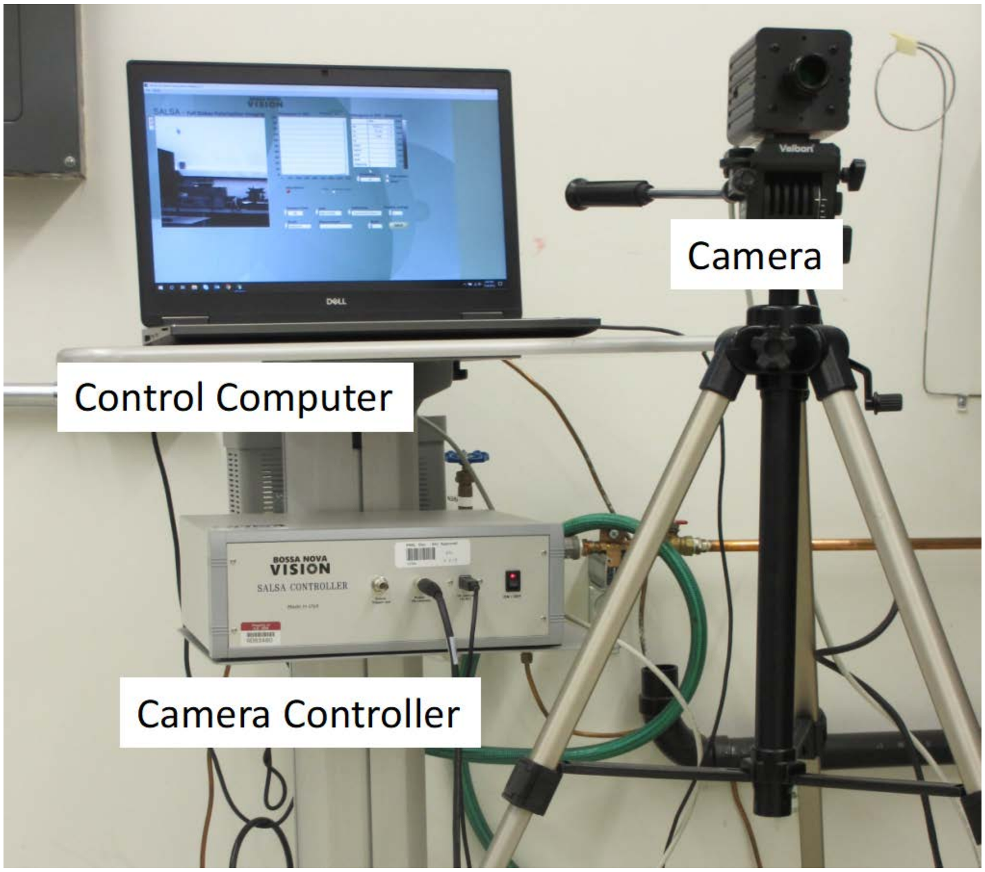

Figure 1.1. Salsa Camera System

2.0 General Images

To appreciate the information the images display, a brief review of polarized light is necessary. When light reaches the surface of a material, it is partially transmitted and reflected. How the light is changed by the interaction includes a great deal of information about the material. Most of light we measure and perceive is reflected from our surroundings. A commonly encountered aspect of polarization and reflection is glare from smooth horizontal surfaces. Glare is polarized orthogonal to the reflecting surface and is removed by only allowing vertically (parallel) polarized light to reach the viewer. This is the basic principle of polarized sunglasses.

The Stokes parameters were developed to mathematically express the polarization of traveling light waves and these four parameters completely characterize the polarization state of light in a compact manner. Each parameter is a vector that captures the light polarization relative to the direction of travel. Born and Wolf (2002) provide detailed information on the Stokes parameters (S0, S1, S2, and S3). Figure 2.1 shows several polarization states for light travelling out of the page toward the reader.

Simply defined, S0 is the sum of the horizontal and vertically polarized light (total intensity), S1 is the difference between the intensity of the vertically (90°) and horizontally (0°) polarized light, S2 is the intensity of light polarized at +/-45° to the vertical and horizontal directions, and S3 is the difference between right and left hand circular polarization. S3 is non-zero when light is partially transmitted through a material with non-isotropic optical properties. Figure 2.1 illustrates several aspects of polarized light.

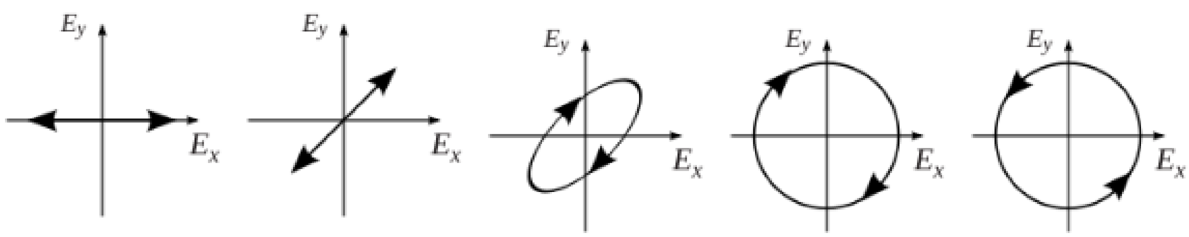

Figure 2.1. Schematic of Polarized Light Traveling out of the Page Toward the Reader. From left to right: horizontally polarized, 45° polarized, elliptically polarized, left-hand polarized and right-hand polarized. The far left image corresponds to the S1 Stokes parameter and the next image is S2. The two far right images represent S3 vectors of opposite sign. The center image is a mixture of non-zero Stokes vectors.

2.1 General Outdoor Images

The Salsa camera can save and export the four Stokes vectors for each image pixel. Colors can be assigned to the Stokes vectors or their magnitude to aid in visualization. Figure 2.2 shows a general outdoor scene imaged with the Salsa camera and a blue filter for each of the Stokes parameters. The S0 image looks like a regular black and white photograph. The S1 image emphasizes smooth manmade surfaces. The S2 image highlights the windshield curves and the S3 image has less contrast but also highlights the windshields as light reflecting from these surfaces displays phase changes. Phase changes occur when the light is significantly altered by traveling through a material. The S1 and S3 images include features in the vehicle interiors that are not discernable in the other images. False colors can be assigned to the Stokes parameters to display several parameters in a single image (Figure 2.3).

Post-processing with ENVI software (L3Harris Geospatial) performs pixel-by-pixel computations on the Stokes parameters provided by the Salsa. Mathematical operations on the Stokes parameters can bring out more detail in the images (Figures 2.4 and 2.5)

2.2 General Indoor Images

A laboratory chemical hood was chosen for indoor imaging. The red, blue and green filters were used with various lenses and camera settings. The complete set of parameters and conditions tested is given in Appendix A. The blue and green filters gave the most polarization contrast and the green filter required the least gain adjustment for the detector.

Dust, scratches and corrosion are readily visible in the polarized images with S1 and S2 showing the most detail. Figure 2.6 shows most of the hood sill. Note the strong signals from the right-angle pipe in the lower left of the images. The polarized images enhance dust, scratches and finger and handprints on the metal sill. Figure 2.7 includes close-up images of the same sill. It includes the area at the left of the images in Figure 2.6. Figures 2.6 and 2.7 are from the Salsa system with no post-processing. Figure 2.8 shows before and after images of a fingerprint on the metal sill. Post-processing with the ENVI software separates the fingerprint details from scratches on the metal surface. As work with the camera progressed, the information content of the S3 parameter generally appeared to be less valuable than the other Stokes parameters. The S3 parameter was only significant when imaging a transparent or translucent coating on top of another material such as the metal sill. Figure 2.9 compares the four Stokes parameter images with an ENVI processed image. The S3 image shows the least amount of detail.

Images were also taken of the same scenes with an infrared camera to verify that the Salsa images were not dominated by emissivity differences between the various materials in the images. The infrared images did not show such dramatic differences between surface defects, handprints or powders and the metal sill.

Figure 2.2. (From left to right) S0, S1, S2, and S3 Polarization Images of the Same Scene. S1 is strongly associated with reflections off the windshields and car hoods while S2 is dominant on the slightly curved windshield edges.

Figure 2.3. Data from the images in Figure 2.2 combined as false colors. Left - S0=red, S1=green and S2 = blue; Right – S1=red, S2=green, S3=blue. Windshield reflections exhibit the most polarization effect and are strongly associated with S1, as expected.

Figure 2.4. Principle Components Analysis of Salsa Images using ENVI Software Showing Greater Detail than the Pure Stokes Images.

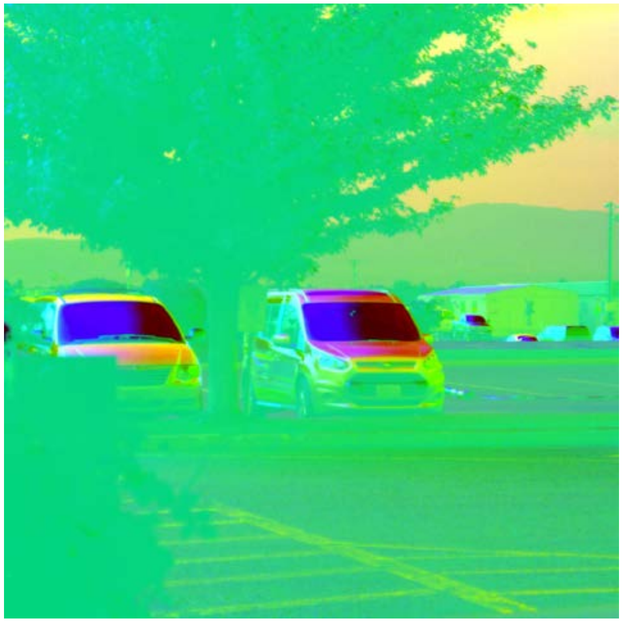

Figure 2.5. False Color Image Created from the Principle Components Images using ENVI Software. This Image uses the first three components from Figure 2.4.

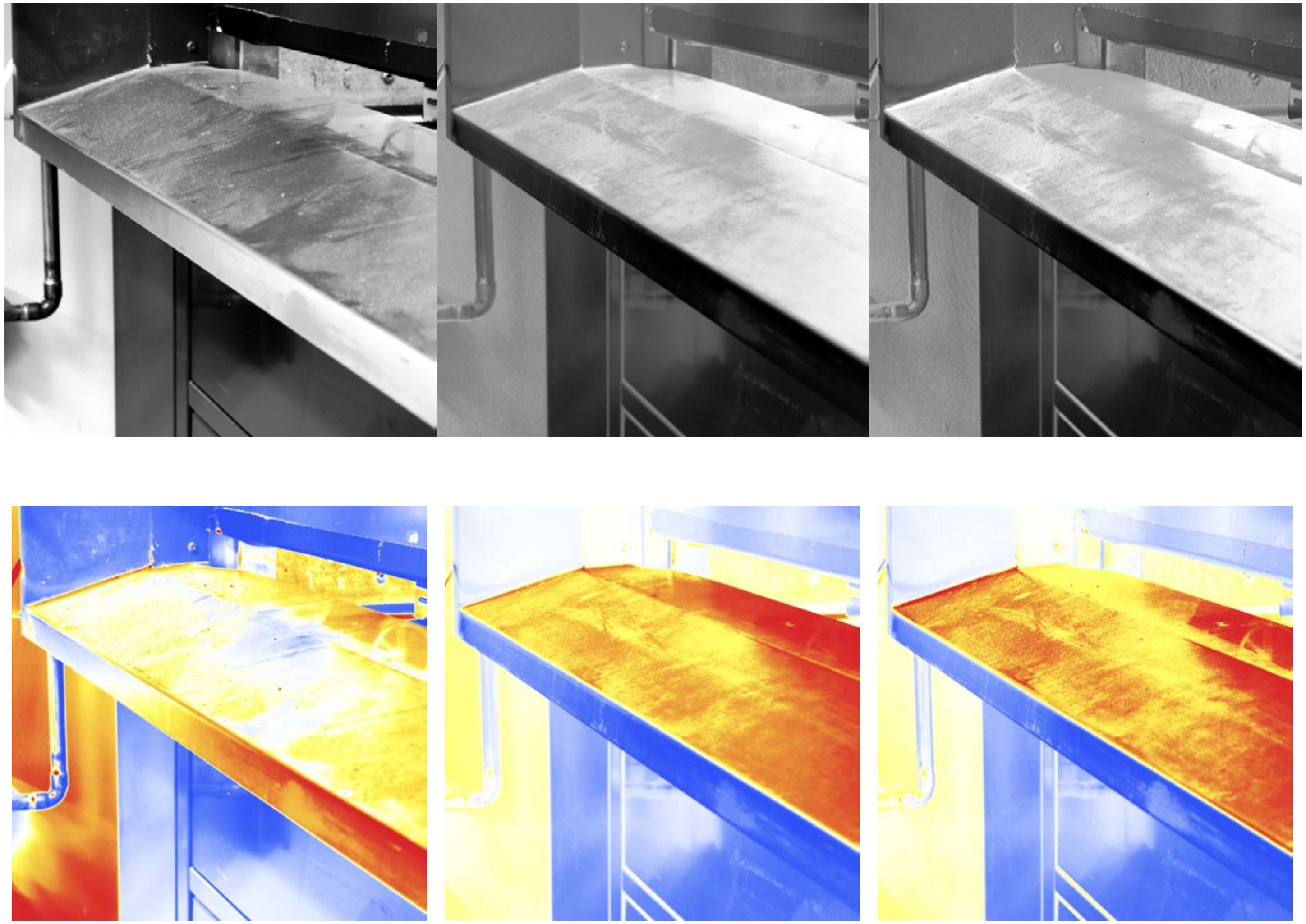

Figure 2.6. S0, S1 and S2 (left to right) Images of a Laboratory Chemical Hood Sill (blue filter). The top row shows standard images and the bottom row presents the same images with false color.

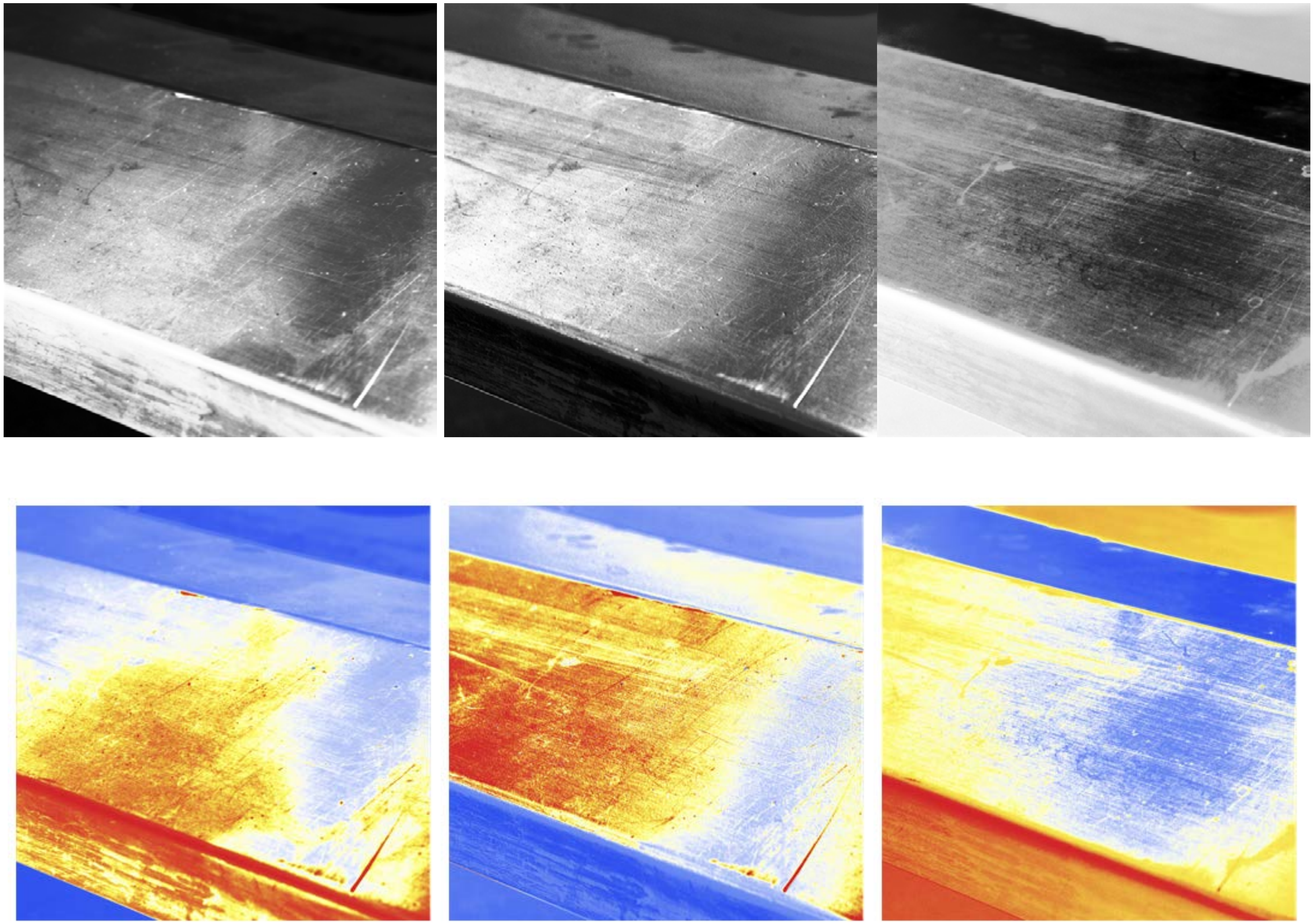

Figure 2.7. From left to right, S0, S1, and S2 Images of a Laboratory Hood Sill. The S1 images show fingerprints on the upper portion of the sill. The S2 image has the impression of a hand-print showing as blue in the false color image. The top row contains normal images and the bottom row contains images with false color.

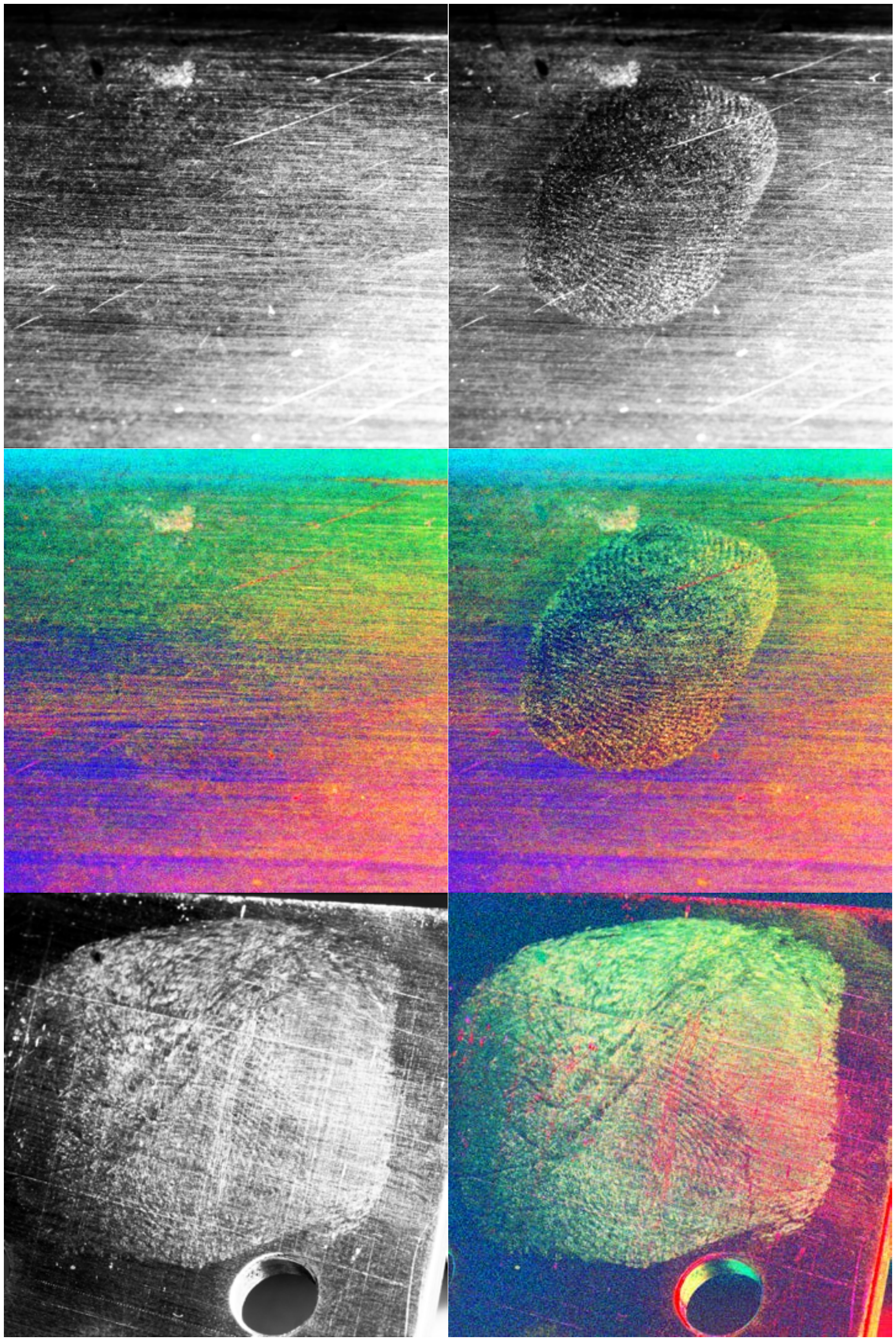

Figure 2.8. Images Before (upper left column) and After (upper right column) Adding a Fingerprint to the Metal Sill. The top row is the S0 image. The second row is the ENVI processed false color image of the corresponding top row images using S0, degree of linear polarization (DOLP), and degree of circular polarization (DOCP) (calculated) values. Bottom row left is the S0 image. Bottom row right is the S0, DOLP and DOCP. Note the metal scratches are red and the fingerprint is mostly green in the lower right image.

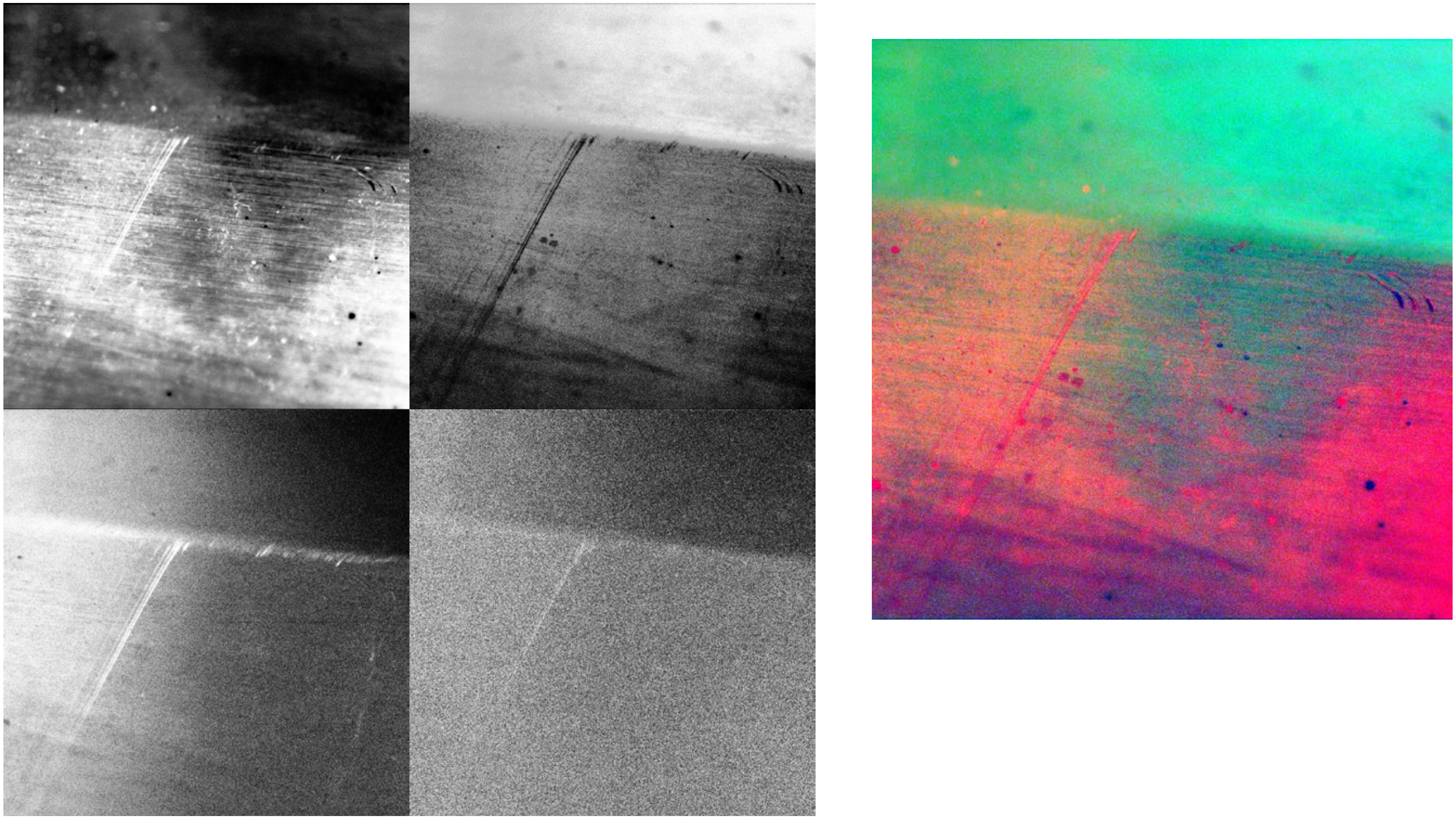

Figure 2.9. Comparison of Black and White and False Color Images. For the black and white images: the top left is S0, top right is S1, bottom left is S2, and bottom right is S3. S3 consistently had less detail than the other Stokes images. The color image is post-processed using ENVI and uses S0, DOLP, and DOCP.

3.0 Powder Images

Rare earth oxide and other powders were applied to various surfaces to determine the impact of polarization imaging. Figure 3.1 shows pale blue neodymium oxide powder rubbed into the painted textured surface of an electrical enclosure. The powder was difficult to see with the unaided eye or in a conventional digital photograph. However, it was easily found in the polarized images.

Figure 3.1. Neodymium Oxide on a Painted Electrical Box. The powder was rubbed into the textured paint in the area just below the metal pointer. The left image is a regular color photograph. On the right is a polarized image of the same area.

Figure 3.2 is of the same neodymium oxide powder on the metal laboratory hood sill. It shows false color images and one ENVI-processed image where the S3 component has the poorest contrast. False color images made using S0, S1, and S2 are comparable to images post-processed using the ENVI software. Figure 3.3 shows the same image data as Figure 3.2 but as processed by ENVI into principle components. The ENVI software can perform multivariate image analysis. The principle component analysis mathematically maximizes the variance or differences in the image data that may not align with the Stokes coordinates. Figure 3.4 shows the same image where the S0 and S2 values were plotted and a region of interest identified that represents the powder on the upper (horizontal) part of the sill.

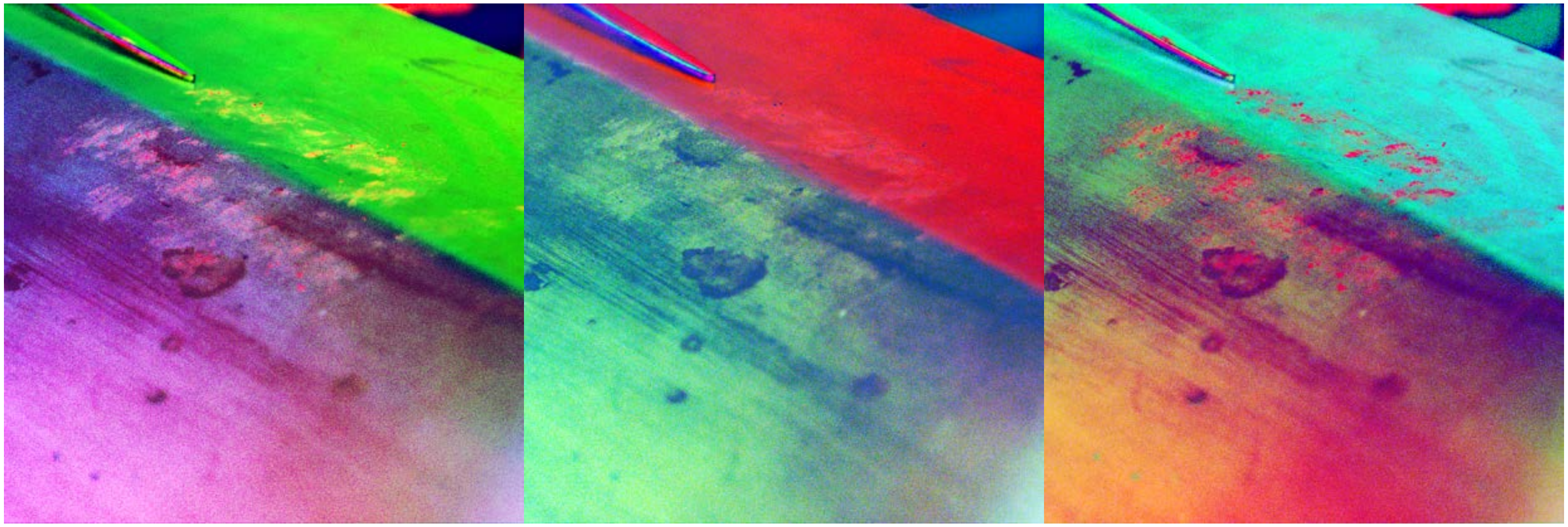

Figure 3.2. False Color Images of Neodymium Oxide Powder on the Metal Hood Sill. The left image shows S0, S1, and S2. The middle image shows S1, S2, and S3. The right image shows S0, DOLP, and DOCP. S3 does not enhance the image contrast.

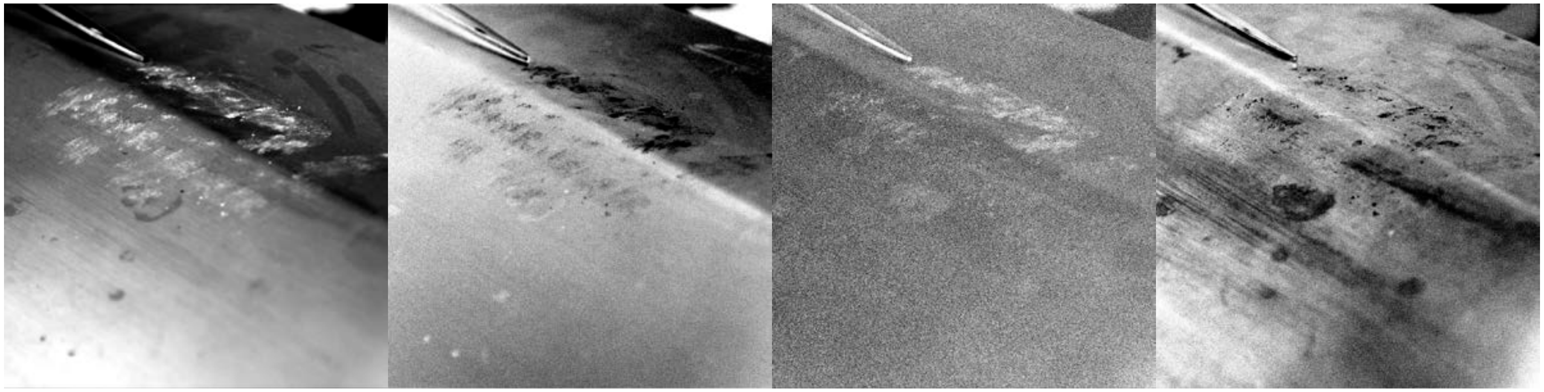

Figure 3.3. ENVI-processed Images Using the Salsa Output. Principle components one through four are the mathematical extremes of the variances of the input vectors (Stokes parameters).

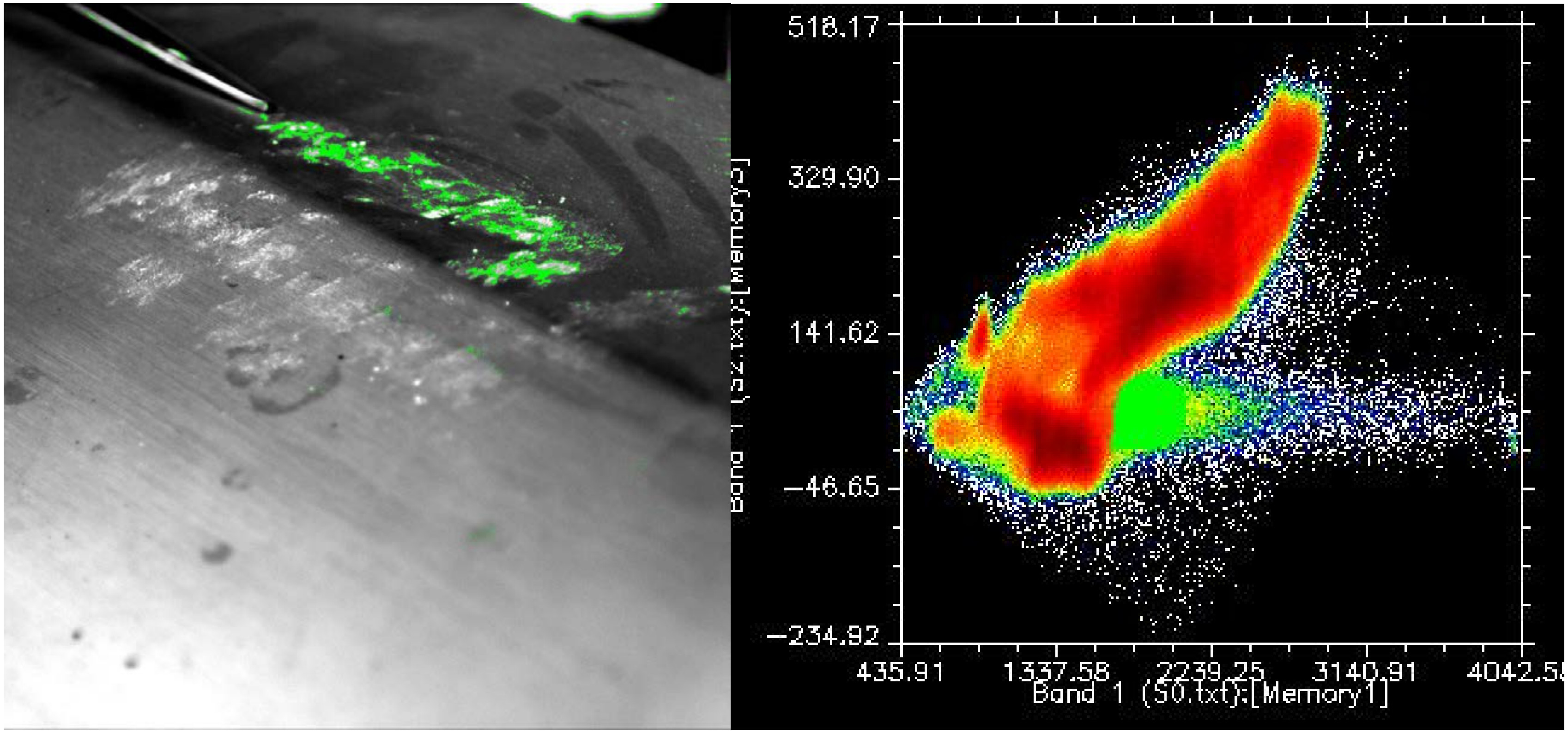

Figure 3.4. ENVI-processed Image Using Multivariant Image Analysis. On the right is the scatter plot of the S0 and S2 values from the Salsa image. The green region in the right-hand plot selects the pixels in the image that have similar attributes.

This page intentionally left blank.

4.0 Semiquantitative Images

Sandpaper was used to obtain information on particle size and how the images are affected. Commercial sandpapers have carefully controlled particle sizes. A set of black (silicon carbide) papers in a series of grits was obtained. The papers were cut into small squares for imaging (1 in^2). Grit size standards vary slightly among the United States (whose standards are American National Standards Institute [ANSI] and Coated Abrasive Manufacturers Institute [CAMI]), Europe (whose standard is Federation of European Producers of Abrasives [FEPA]) and Japan (whose standard is Japan Industrial Standards [JIS]). The set used in this study appears to be Japan standard grits. Grits are defined by the sieves they can pass through and the average particle size is given as the mean spherical diameter. The sandpapers shown are 1500, 600, 240, and 120 grit, which correspond to mean particle sizes of 12, 20, 60, and 125 microns.

Figure 4.1 shows sandpapers under three different camera settings. S2 shows the most contrast among the four papers. S1 shows the hand-written labels in the greatest contrast. All the images used the green filter and the bottom row had the longest exposure time of 100 ms, f--stop of 1.4, and low gain on the detector. Figures 4.2 and 4.3 are the sandpaper groups rotated relative to the camera to verify that the differences in Figure 4.1 were not caused by lighting effects. Figure 4.2 includes an additional light source while Figures 4.1 and 4.3 used the ambient lighting of the laboratory. The strong contrast between the sandpapers for S2 is consistent regardless of the lighting source or orientation to the camera. The blue and green filters gave comparable results.

In optics the refractive index and thickness tend to be intimately combined, and in most transmission or reflection measurements one must be known to calculate the other. The Fresnel equations address this issue if many measurements can be taken at several fixed geometries. The sandpapers could be differentiated in the S2 images without post-processing. This indicates that the images are sensitive to differences in particle size for a single grit material. However, both the optical properties and particle size of the grit affect the light. Two sets of images were collected on white or nearly white powders to test if optical properties or particle size dominated the polarized images. The authors had ready access to chemicals of known refractive index, but unknown particle size and a separate group of chemicals with similar refractive index but known particle sizes. Each group was imaged after rubbing a small amount onto sandpapers.

Figures 4.4 through 4.7 are white powders (neodymium oxide is a very pale blue) of known refractive index smeared onto sandpaper. Cerium oxide and neodymium oxide were used as high Z oxide powders. The other powders were magnesium oxide (n=1.7) and lithium carbonate (n=1.47). The samples were rotated to determine any ambient lighting effects. Figure 4.4 shows that the polarization of the lithium carbonate and magnesium oxide are distinctly different from each other and the blank sandpaper. In Figure 4.5 the center sandpaper square is smeared with cerium oxide. Figure 4.6 has neodymium oxide in the center. The four powders image differently. Without particle size information it is not conclusive that the images are entirely due to refractive index differences.

Another set of images was taken to address the impact of particle size. These images are shown in Figure 4.7. Sized powders of silica (SiO_2) and alumina (Al_2O_3) were available. Their refractive indices are ~1.5 and ~1.7 respectively (both materials are optically anisotropic). The silica size fractions were less than 50 um, 45 to 75 um, and 75 to 125 um. The alumina size fractions were 50 um, 125 to 180 um, and 180 to 250 um. These powders were also smeared onto sandpaper squares. Several of the powder smears are difficult to see in a conventional digital photograph. Figure 4.8 shows that S0 appears to be affected by the thickness of the smear, S1 has little information, and S2 and S3 show the most contrast between the different particle sizes. Post-processing was performed on the top row images in Figure 4.7 using the ENVI software. The results are in Figure 4.8. It appears that in both Figures 4.7 and 4.8 the finest particle sizes show more distinct polarization behavior. Both silica and alumina are optically uniaxial with two distinct polarization directions for transmitted light. If the small particles partially transmit and then reflect light back to the camera this would explain the more significant values in the S3 images.

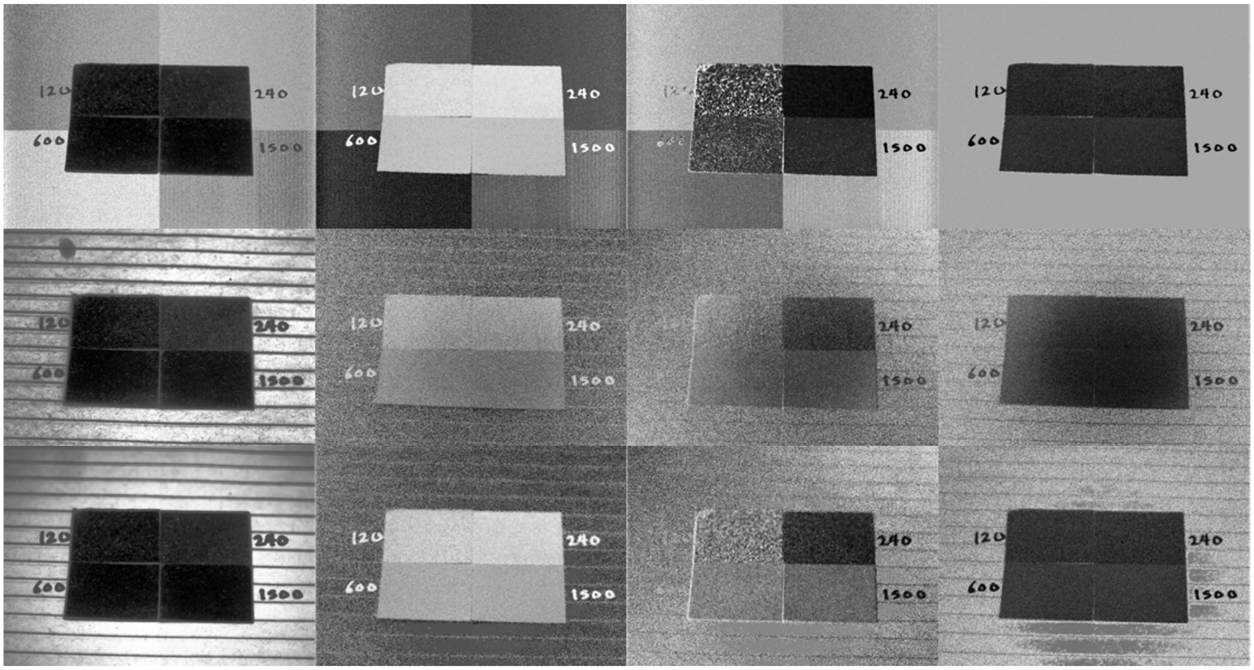

Figure 4.1. (Left to right) S0, S1, S2, and S3 of Various Sandpapers with the Grit Size Handwritten on Lined Paper (120, 240, 600, and1500). Each row used the green filter and varied f-stop, integration time, and gain.

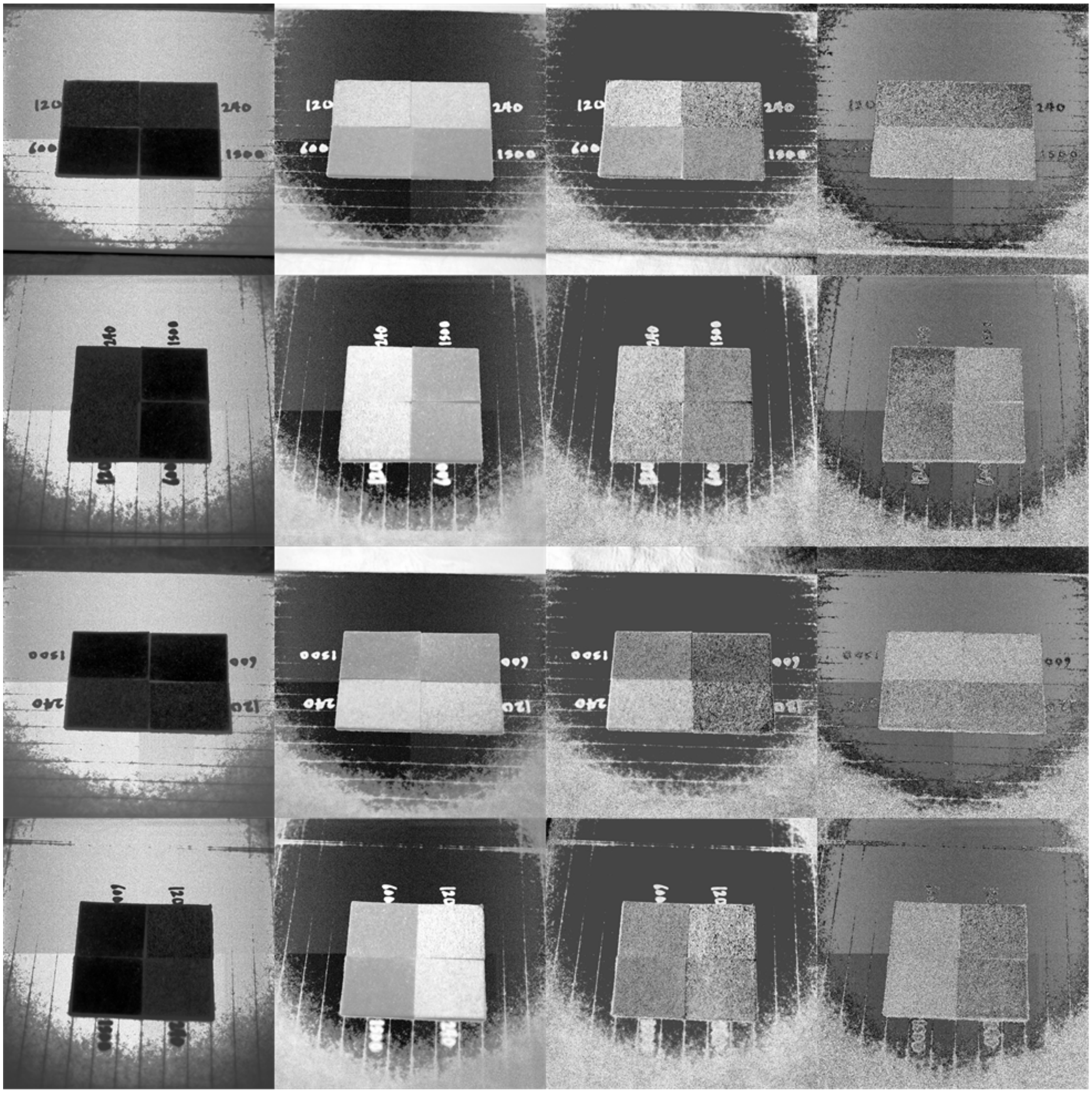

Figure 4.2. The Same Four Sandpapers as in Figure 4.1 with Supplemental Lighting. From left to right is S0, S1, S2, and S3. Each horizontal row is a different orientation to the camera.

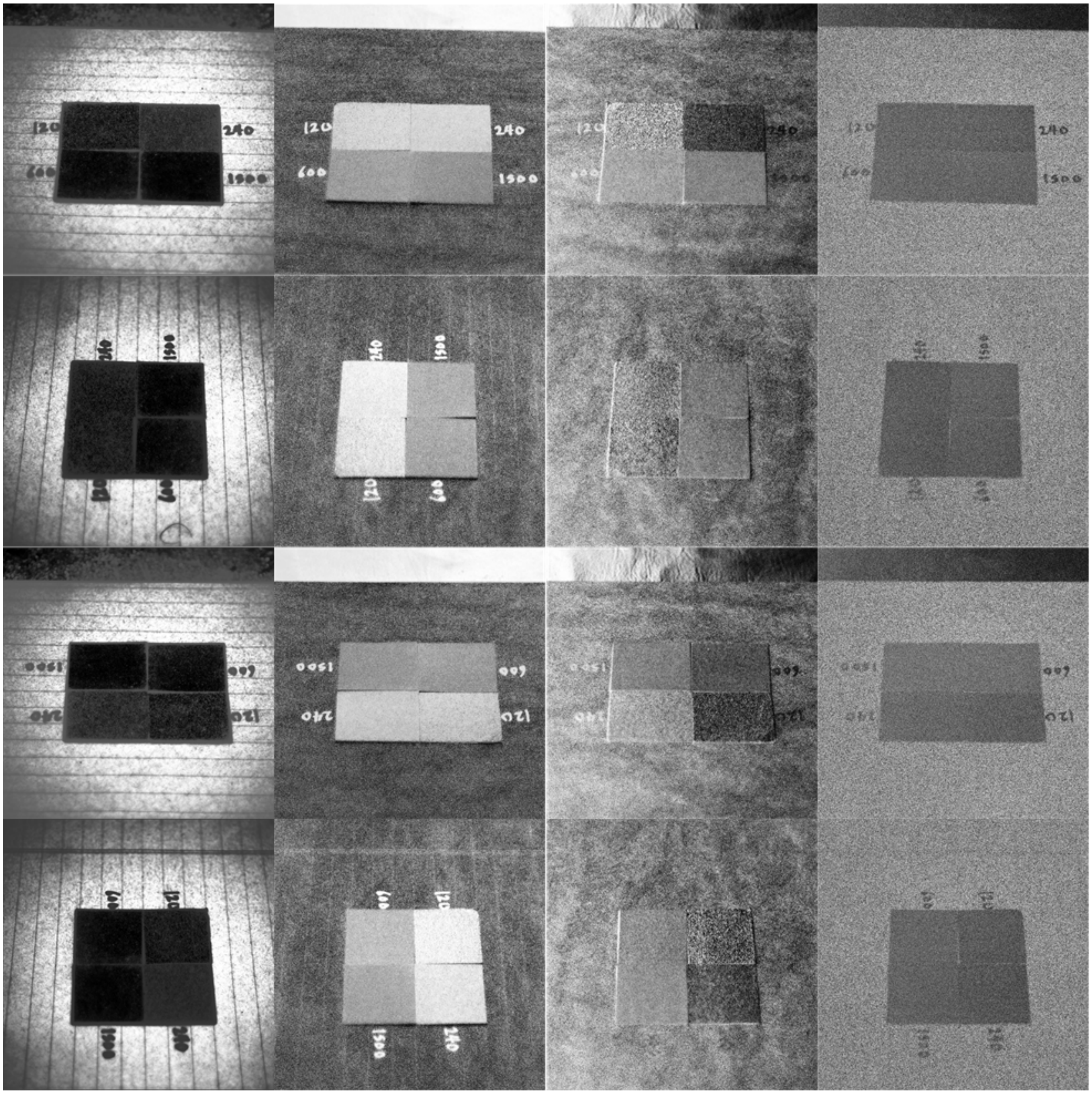

Figure 4.3 The Four Sandpaper Squares at Different Orientations Under Ambient Lighting. Left to right is S0, S1, S2, and S3. Each row is a different orientation relative to the camera.

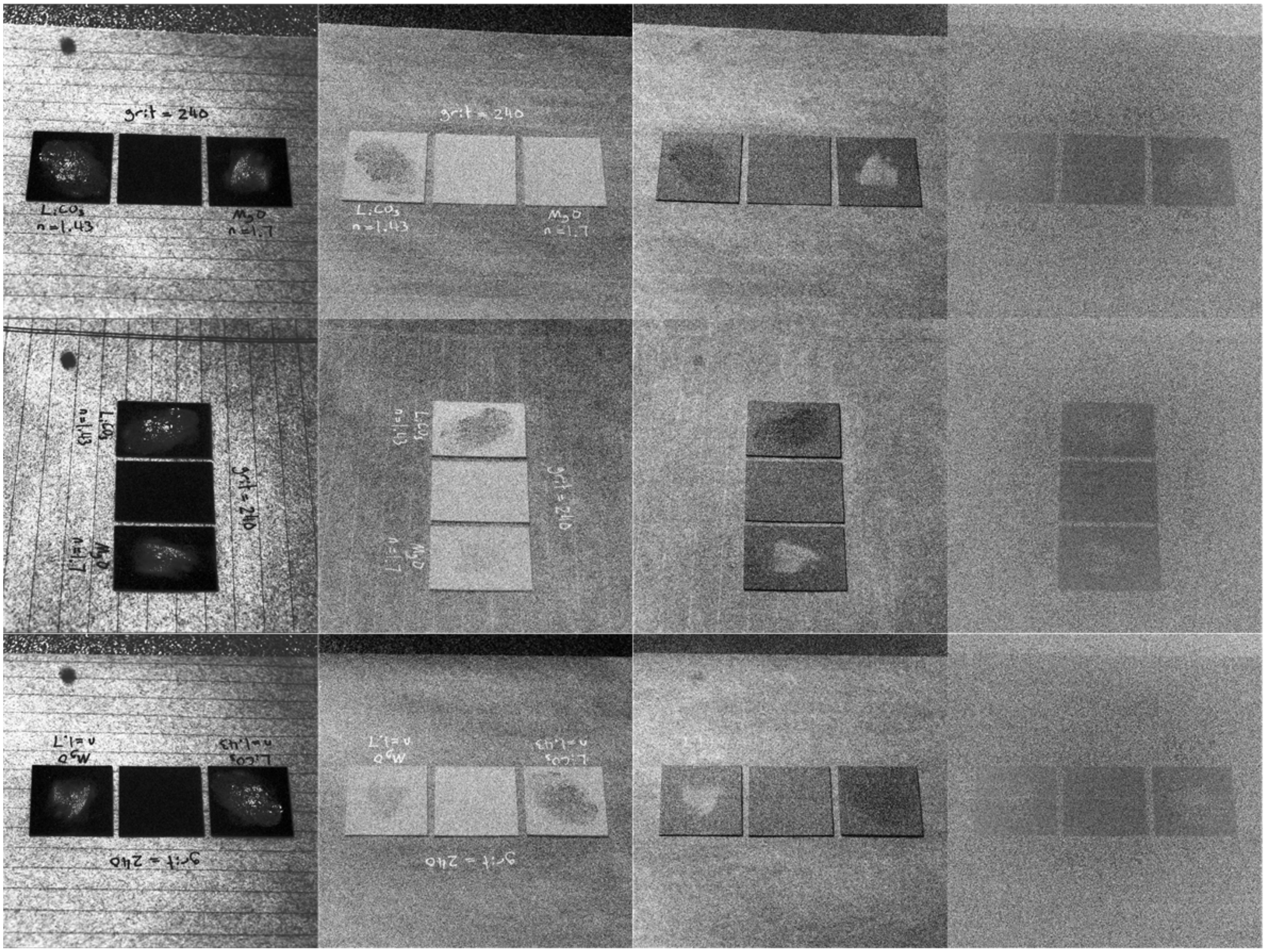

Figure 4.4 The polarization of Lithium Carbonate and Magnesium Oxide are Distinctly Different from each Other and the Blank Sandpaper. Left to right are S0, S1, S2 and S3. Top row is 240 grit sandpaper with smears of lithium carbonate and magnesium oxide. The center piece is bare sandpaper. The middle and bottom rows are orientation changes relative to the camera.

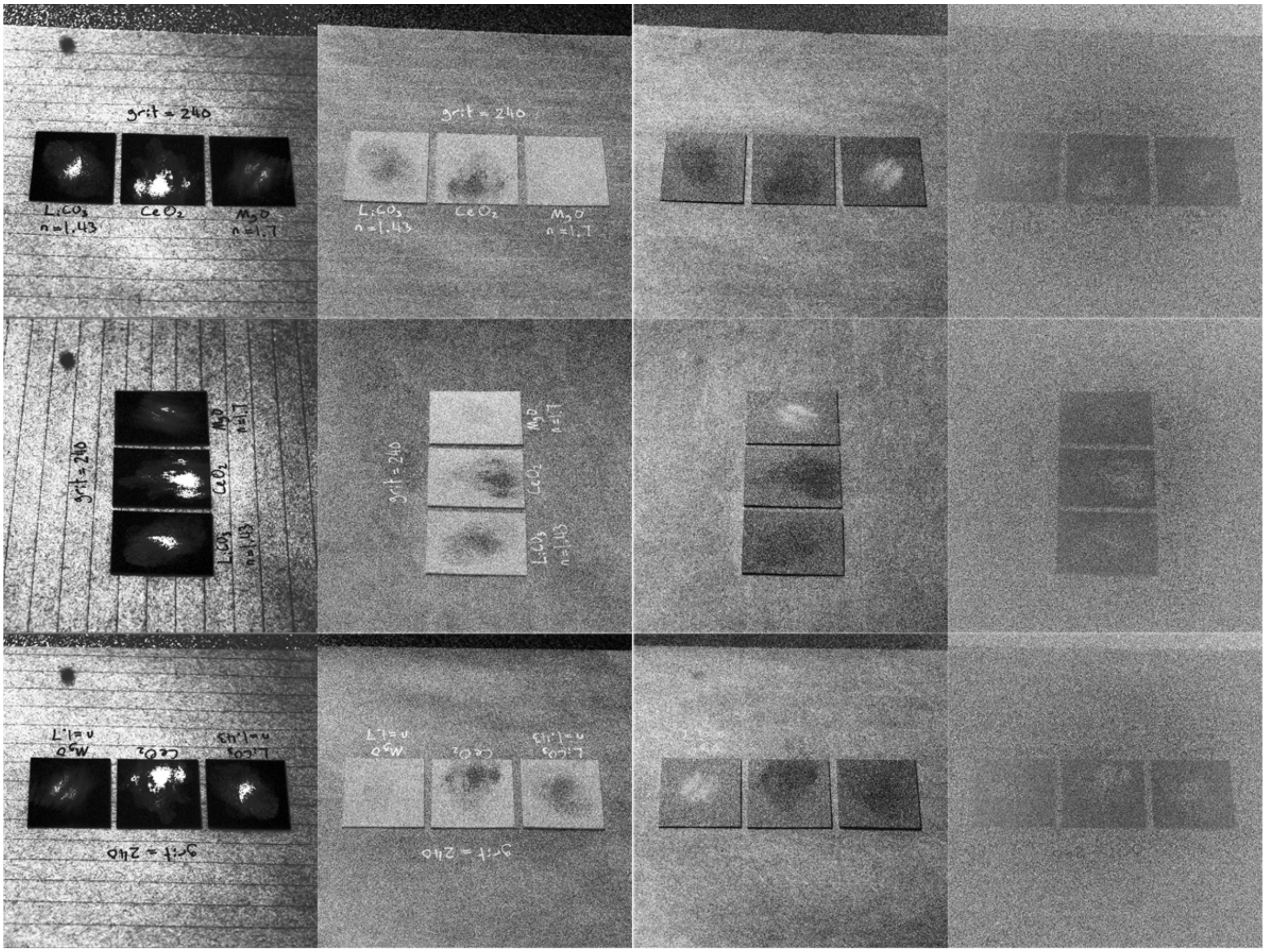

Figure 4.5. The columns (from left to right) show S0, S1, S2 and S3 images of 240 Grit Sandpaper Smeared with Lithium Carbonate, Cerium Oxide (center), and Magnesium Oxide. Each row is at a different orientation to the camera and light source. The S3 images show the least contrast.

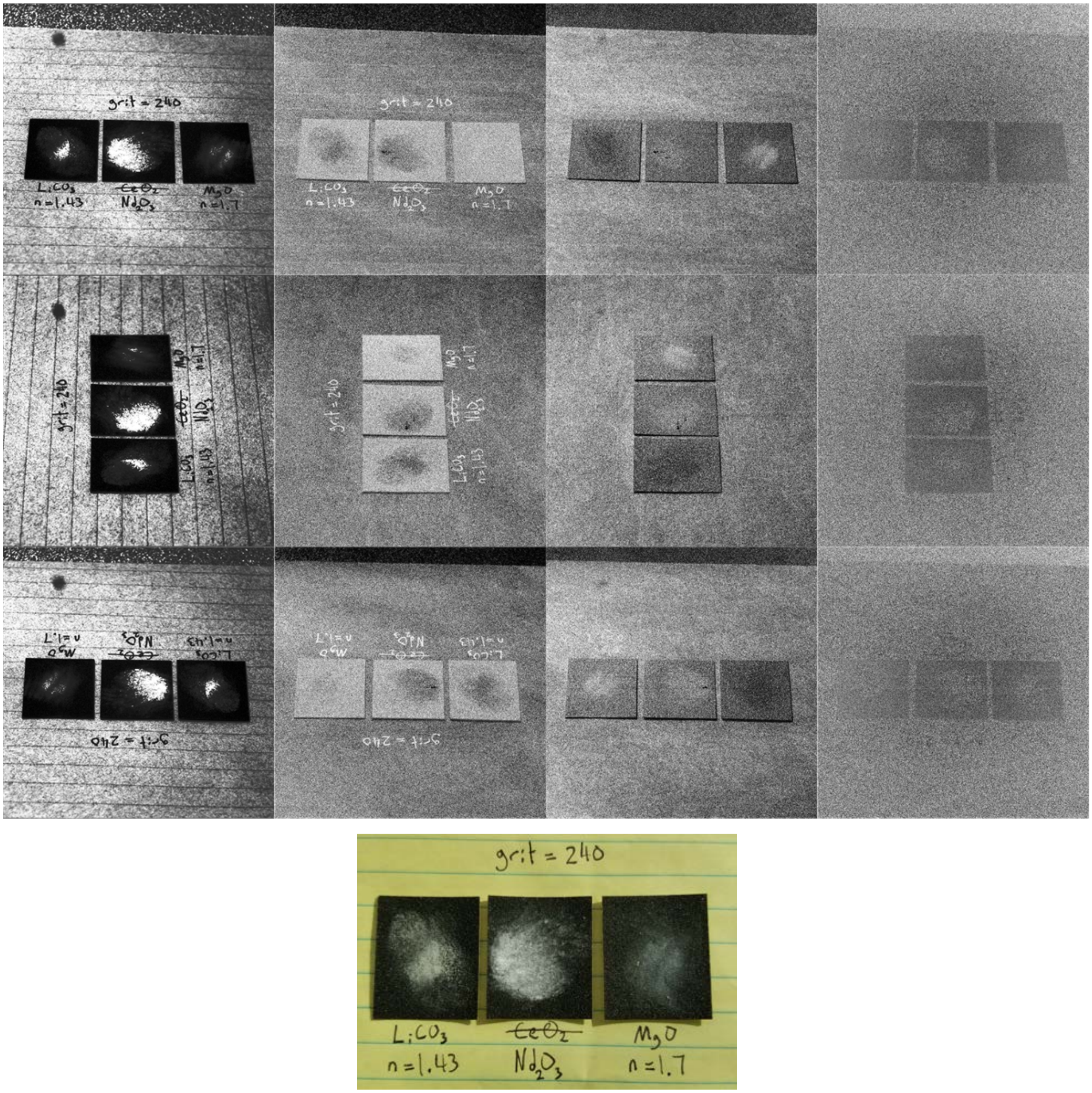

Figure 4.6. 240 Grit Sandpaper Smeared with Lithium Carbonate, Neodymium Oxide and Magnesium Oxide. The neodymium oxide is in the center square. The columns (left to right) show S0, S1, S2, and S3 images. The rows are at different orientations to the camera and ambient lighting. The bottom image is a digital photograph of the samples.

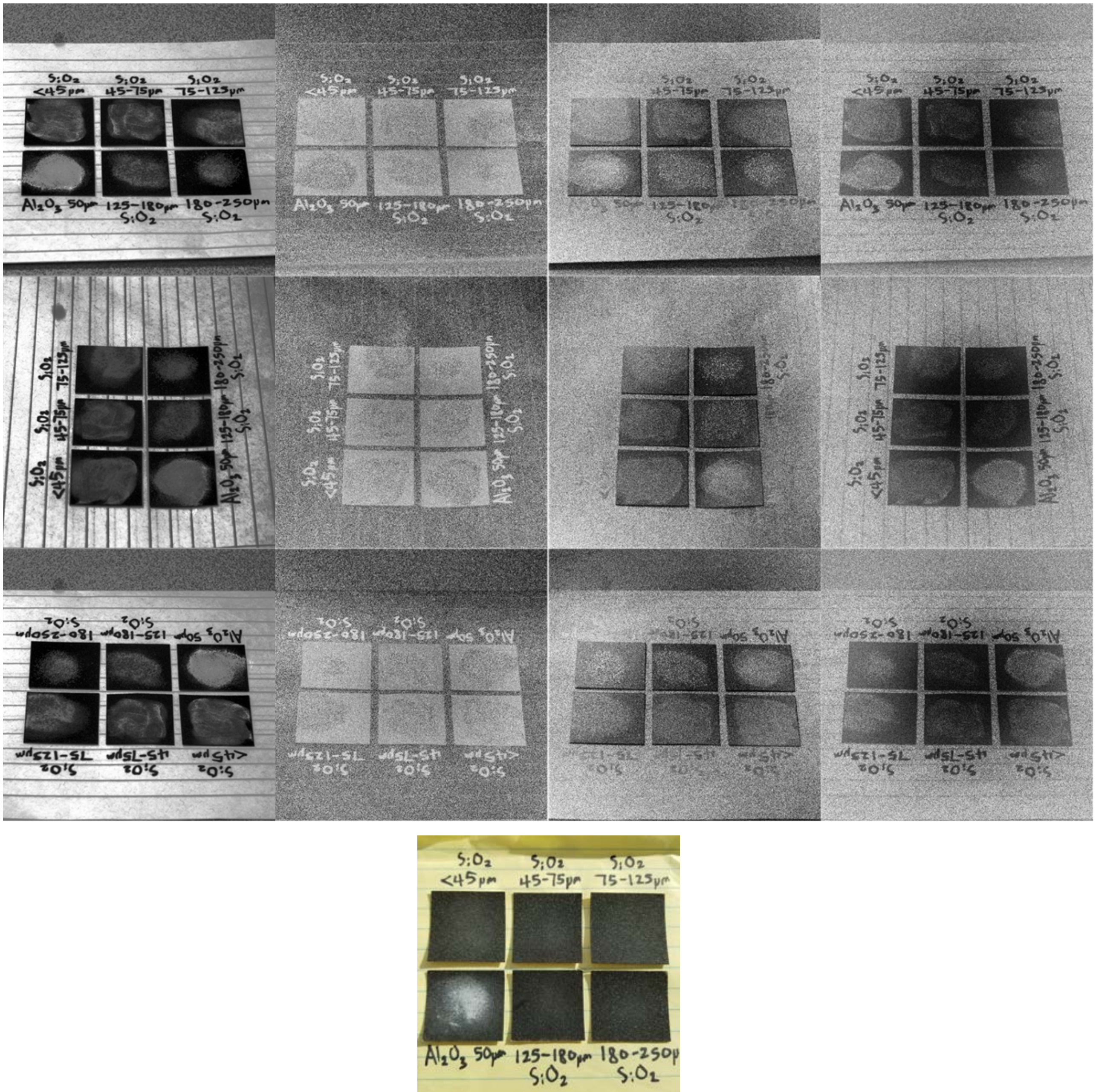

Figure 4.7. Silica and Alumina Smears on Sandpaper Sorted by Particle Size. The columns (left to right) show S0, S1, S2 and S3 images and the rows are of different orientations to the camera and light source. The bottom image is a digital photograph of the samples.

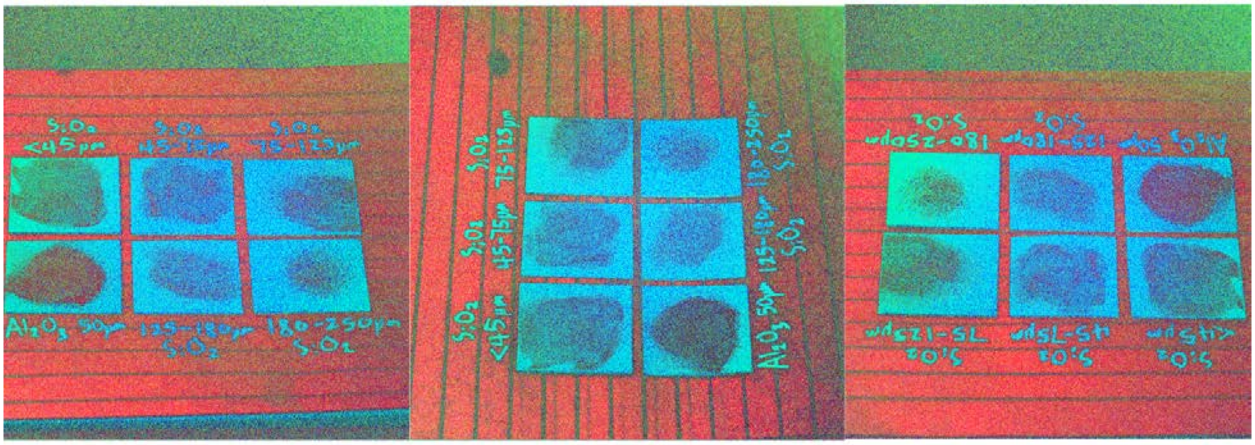

Figure 4.8. Post-processed False Color Images of the Smears in Figure 4.7. S0 = red, DLOP = green, DOCP = blue. Both silica and alumina are optically uniaxial, and the circular polarization effect may be attributed to light that is transmitted through the particles and then reflected to the camera.

5.0 Uranium Oxide Particles

One-micron uranium oxide particles, from other work at PNNL, were examined. These particles were developed as standards for the IAEA. Three different concentration suspensions were pipetted onto a glass slide (2 x 2 in.) and dried. The dried particles adhere to the glass slide and become fixed. The slide is not radiologically controlled material when prepared in this manner. The dried dots are millimeter-sized. The Salsa camera could not image the dried particles on the slide. Figure 5.1 shows the glass slide on which the three dried dots are above the flat side of the half circle marker. The graininess of the image is attributed to the surface below the slide. The camera was focused on the half circle marker so that the top of the slide was also in focus.

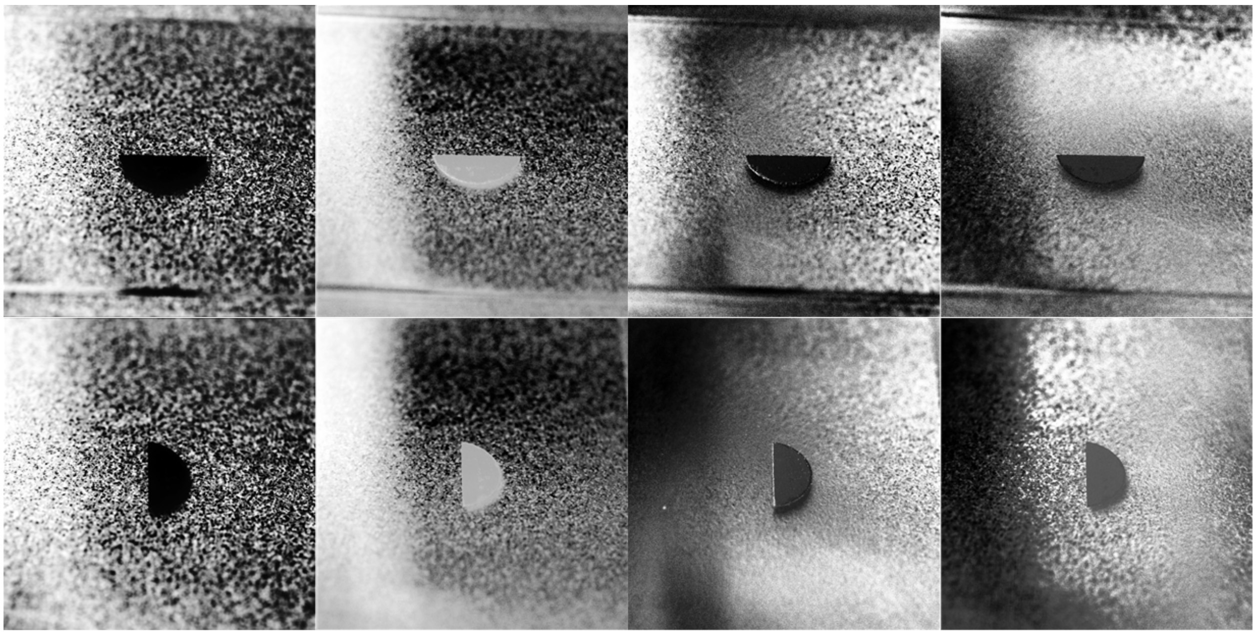

Figure 5.1. Uranium Oxide Particles on a Glass Slide. On the top row, the dried particles are above the flat side of the semicircle and on the bottom row they are to the left of the semicircle.

This page intentionally left blank.

6.0 Conclusions

The Salsa camera performed well and met all the procurement specifications. It is easy to use. The raw image data could be exported and analyzed using other software. The images are rich in information but, as with any camera system, the field of view is important.

Magnification and depth of field are controlled by the lens system. The Salsa can accommodate many commercial lenses, but lens selection relies on the expertise of the operator. The 12 fps imaging rate was adequate for real-time video operation. Only one polarization state at a time is available in video mode. A tripod is needed for long exposures.

Longer and co-added exposures reduce the detector gain which improves dynamic range in the image data. The number of co-added images is limited to 10, which appears to be a software or memory limitation of the system. The Salsa camera did not require additional light sources and worked well under ambient office and laboratory lighting.

The polarization images are very sensitive to texture and surface finishes. Powders in moderate quantities appear distinctly in the polarized images. Different chemicals appeared different from each other in the polarized images. This is related to both refractive index and particle size (as expected). The fine alumina and silica powders readily showed in the polarized images but were difficult to see with the unaided eye and a digital camera. These larger deposits of transparent powders (silica and alumina) were much more visible in the polarized images. The critical limitation of the imaging system is that the dilute uranium oxide particles could not be imaged.

The uranium oxide particle deposits were difficult to see on the glass slide with the naked eye and an inspection microscope. The Salsa camera had comparable difficulty. For minute amounts of material, that are typical of swipe sampling, the camera does not offer a significant advantage in finding small deposits on a smooth surface. The figures in Section 2.2 show that the imager can document dirt and scratches on large surfaces. This may aid in documenting large areas for environmental swiping, but there is no significant advantage in locating very small deposits. The polarization imager was very useful in highlighting powders on textured surfaces.

The sensitivity to texture and lack of ambient lighting sensitivity make polarization imaging for tamper indication viable. Further investigation into tamper indication is warranted. It is also worth noting that polarization imagers are useful for removing reflections from water or windows. Some of the images in Section 2.1 show features inside the passenger cars. Polarization imaging may be useful for inspecting nuclear reactor ponds, spent fuel storage ponds or glove boxes used for materials processing.

Conventional cameras have significant issues with glare when imaging water or windows. Simple linear polarization cameras would be useful in these cases based on our experience with the Salsa system. The full Stokes parameters would be useful in discriminating smears from other materials. The optical effects are quite complex and may require extensive post-processing.

The comparison of refractive index and particle size indicate that a series of images could be post-processed to estimate optical properties or particle size. Even if a rigorous Fresnel equation analysis was not possible, artificial intelligence image analysis methods could be trained on known powders. Ideally, this would offer estimates of refractive index and particle size that would aid in material identification without having to contact or remove the sample.

This page intentionally left blank.

7.0 Bibliography

Born M and E Wolf. 2002. *Principles of optics*. 7th Edition, Cambridge University Press, Cambridge, United Kingdom.

Bossa Nova Vision. 2018. *Salsa Full Stokes Polarization Imaging Software Users Manual*, *Version 2.3.7*. Bossa Nova Vision, Los Angeles, California.

Bossa Nova Vision. 2018. *Salsa Software Development Kit*. Bossa Nova Vision, Los Angeles, California.

Cremer F, W de Jong, K Schutte, W-J Liao, and BA Baertlein. 2003. “Detectability of surface-laid landmines with a polarimetric IR sensor.” *Proceedings of SPIE Vol. 5089, Detection and Remediation Technologies for Mines and Minelike Targets VIII*. RS Harmon, JH Holloway, Jr., and JT Broach, eds.

Dollfus A. 1998. “Lunar Surface Imaging Polarimetry: I Roughness and Grain Size.” *Icarus*, 136:69-103. Article No. IS986008.

El Ketara M, M Vedel, and S Breugnot. 2016. “Acquisition method improvement for Bossa Nova Technologies' full Stokes, passive polarization imaging camera SALSA.” *Proc. SPIE 9853, Polarization: Measurement, Analysis, and Remote Sensing XII,* David B. Chenault, Dennis H. Goldstein, eds. DOI: 10.1117/12.2224357.

Hsu WL, G Myhre, K Balakrishuau, N Brock, MI Elhaj, and S Pau. 2014. “Full-Stokes imaging polarimeter using an array of elliptical polarizer.” *Optics Express*, 22(3). DOI:10.1364/OE.22.003063.

Joardar S. "Polarimetry." Presentation.

"Polarization of Light: circularly polarized, linearly polarized light". https://www.youtube.com/watch?v=8YkfEft4p-w (accessed February 7, 2020)

"Polarization of light, linear and circular" https://www.youtube.com/watch?v=HH58VmUbOKM (accessed February 7, 2020).

Qi J, C He, and DS Elson. 2017. "Real time complete Stokes polarimetric imager based on a linear polarizer array camera for tissue polarimetric imaging." *Biomedical Optics Express*, 8(11). https://doi.org/10.1364/BOE.8.004933.

Smoke JA. 2017. *Comparison of polarimetric cameras*. Master of Science Thesis. Naval Post Graduate School, Monterey, California. http://hdl.handle.net/10945/53050.

Tu X, OJ Spires, X Tian, N Brock, R Liang, and S Pau. 2017. "Division of amplitude RGB full-Stokes camera using micro-polarizer arrays." *Optics Express*, 25(26). https://doi.org/10.1364/OE.25.033160.

Vedel M, S Breugnot, and N Lechocinski. 2015. "Full Stokes polarization imaging camera." *Proceedings of SPIE Vol. 8160, Polarization Science and Remote Sensing V*. JA Shaw and JS Tyo, eds., DOI: 10.1117/12.892491.

Zhao Y, Q Peng, C Yi, and SG Kong. 2016. "Multiband Polarization Imaging." *Journal of Sensors*, 2016(5985673). http://dx.doi.org/10.1155/2016/5985673.

Appendix A Camera Parameter Tests

Camera Test 1

Parameter	Value
Filter	Green
Integration Time (ms)	?
Gain Setting	Medium
Frames Averaged	5
Angle with surface (deg)	15, 30, 45, 60
Lighting	Ambient

Camera Test 2

Parameter	Value
Filter	**Red, Green, Blue, None (Green Calibration)**
Integration Time (ms)	**?**
Gain Setting	**Medium, Medium, High, Low**
Frames Averaged	**5**
Angle with surface (deg)	**15**
Lighting	**Ambient**

Camera Test 3

Parameter	Value
Filter	Green
Integration Time (ms)	?
Gain Setting	Medium
Frames Averaged	1, 5, 3
Angle with surface (deg)	15
Lighting	Ambient

Camera Test 4

Parameter	Value
Filter	Green
Integration Time (ms)	200, 100, 30
Gain Setting	Low, Medium, High
Frames Averaged	5
Angle with surface (deg)	15
Lighting	Ambient

This page intentionally left blank.

Pacific Northwest
National Laboratory

902 Battelle Boulevard
P.O. Box 999
Richland, WA 99354
1-888-375-PNNL (7665)

www.pnnl.gov